

ICAS 15 - Proceedings of the 15th International Conference on
 AMORPHOUS SEMICONDUCTORS: Science and Technology,
 Cambridge, U.K., 6-10 September 1993
 Edited by: S.R. Elliott, E.A. Davis and J. Robertson
 (to be published as a special issue of the Journal of Non-Crystalline Solids)

High performance acousto-optic chalcogenide glass based on Ga_2S_3 - La_2S_3 systems

I. Abdulhalim, C.N. Pannell, R.S. Deol, D.W. Hewak, G. Wylangowski, D.N. Payne

Optoelectronics Research Centre - Optical Fibre Group
 Southampton University - Southampton, SO9 5NH, U.K.

Chalcogenide glass systems based on Ga_2S_3 - La_2S_3 (GLS glass), have been found to exhibit relatively high acousto-optic figures of merit, low acoustic loss and high acoustic velocity. These properties of the GLS glass combined with its transparency both in the visible and the infrared (0.5-10 μm), nontoxicity, high softening temperature ($T_g = 561^\circ\text{C}$), ease of fabrication, optical quality, chemical stability, and isotropic properties, make it attractive for acousto-optic device applications.

1. Introduction

Conventional chalcogenide glasses such as As_2Se_3 and As_2S_3 are known¹ to exhibit high acousto-optic (AO) figures of merit suitable for building acousto-optic modulators (AOMs), however, they suffer from a number of drawbacks. Their main disadvantages are their high absorption in the visible range (absorption edge $\sim 0.8 - 1.8$ eV), toxicity, low softening temperature (200-300 $^\circ\text{C}$) and low damage threshold. Their photosensitivity to light with photons energy below the absorption edge is another limitation. The chalcogenide glass $\text{Ge}_{33}\text{As}_{12}\text{Se}_{55}$ was found² to exhibit better performance, however it is opaque in the range below 1 μm . The purpose of this article is to show that the chalcogenide glass system based³ on Ga_2S_3 - La_2S_3 (GLS glass) are attractive for acousto-optic applications. They are optically transparent in the range 0.5 - 10 μm (figure 1), have a high refractive index, are non toxic, and their glass transition temperature is higher ($T_g = 561^\circ\text{C}$). The interest in this glass system was awakened recently due to its low phonon energy, hence acting as a promising host for rare earth elements for the development of an efficient optical fibre amplifier operating in the near infrared region.⁴ The GLS glass can therefore be suitable for building efficient in-fibre acousto-optic devices.

2. Experimental

The glass composition we used is $70\text{Ga}_2\text{S}_3$ - $30\text{La}_2\text{S}_3$, and fabricated in our laboratory. The starting powders (Ga_2S_3 and La_2S_3) were placed within glass ampoules whose interior was carbon coated. This carbon coating prevents the glass melt from reacting with the ampoule walls, thus avoiding devitrification from the melt. The ampoules were pumped down to a vacuum of $\sim 10^{-6}$ torr and sealed, then baked in a furnace at 1150 $^\circ\text{C}$ for two hours while being rotated, then removed and quenched in water at room temperature.

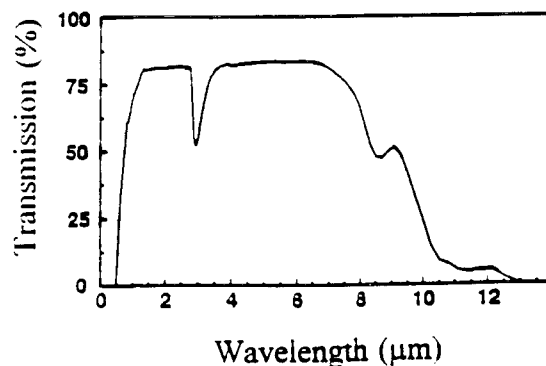


Figure 1. Transmittance spectrum of the GLS glass. The dip near 3 μm is due to OH impurities.

The sample used to build the AOM was polished on its faces down to $\lambda/4$ flatness with dimensions 6x7x10 mm. The fabrication of an AOM from this glass was performed by Gooch & Housego-UK, Ltd. The piezoelectric transducer is a 42 μm thick LiNbO₃, Y-cut at 36° to provide compressional wave at 80 MHz. A 1000 Å thick gold layer deposited on one of the polished faces of the glass with the dimensions 6x10 mm acts as the bottom electrode. On the opposite face a metallic absorber is attached in order to ensure travelling wave operation. The transducer is bonded directly to the gold using the technique of vacuum indium-cold-welding. A matching circuit was connected to the transducer to minimise the reflected RF power at resonance. The lateral dimensions of the transducer are $L = 3$ mm long and $H = 1$ mm wide. Although this length of the transducer is not the optimum which yields 100% diffraction efficiency, we were able to estimate the main acousto-optic parameters of the glass and to predict from these the optimum interaction length.

To characterise the device, light from HeNe laser at $\lambda = 633$ nm launched into a single mode fibre was recollimated at the distal end using a quarter pitch GRIN lens. The output from a single mode fibre was used for two reasons. First, to obtain spatial filtering which is found to improve the diffraction efficiency. Secondly, to achieve a collimated gaussian laser beam with small waist to demonstrate fast switching under pulsed operation. The collimated beam had a waist of $\omega_0 = 143$ μm measured using the knife edge technique.

3. Results and Discussion

Figure 2 shows the variation of the diffraction loss and the diffraction efficiency with the RF power level under CW operation using a collimated HeNe laser beam at 633 nm. The diffraction loss is the ratio between the light intensity in the 0th order beam when the RF signal is ON to that when it is OFF. The diffraction efficiency is the ratio between the light intensity diffracted into the 1st order beam to the transmitted intensity when the RF signal is OFF. Figure 3

shows the variation of the deflection angle β with the acoustic frequency ν . By fitting these measurements to the relation $\beta = \lambda\nu/v$, we determined the acoustic velocity $v = 4365$ m/s.

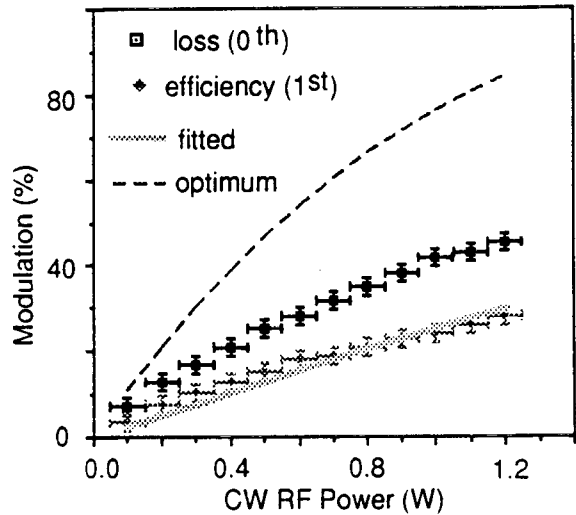


Figure 2. The variation of the measured diffraction loss and efficiency with the RF power. The fitted (thick solid) and optimum (thin solid) diffraction efficiency curves are shown.

The diffraction loss is usually higher than the diffraction efficiency because part of the light is diffracted to other diffraction orders if the AOM is not operating exactly in the Bragg regime.

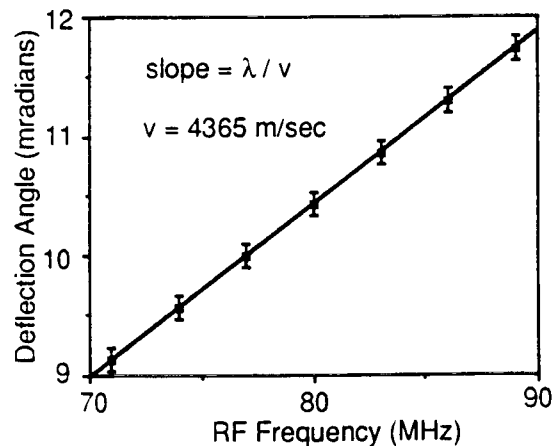


Figure 3. Variation of the measured deflection angle with the RF frequency.

For pulsed operation the RF signal was pulsed with 100 μ s, 80 MHz tone-bursts at 2 kHz repetition rate and average RF power of 0.2 W. Under these conditions we measured a rise time of 46 ns. The optical rise time τ_r is given by Maydan's⁵ formulae: $\tau_r \sim 1.3\omega_b / v$ which with $\omega_b = 143 \mu$ m and $v = 4375$ m/s yields $\tau_r = 42.5$ ns in agreement with the measured value.

The acoustic velocity was estimated from a measurement of the delay time between the RF pulse and the optical response as a function of the beam position from the transducer plane (figure 4). The value of v obtained by this technique is very accurate because the position of the optical beam and the delay time are relative quantities measured with respect to fixed points in space and time domains respectively. The value obtained $v = 4375$ m/sec, agrees with the value estimated from the measurement of the deflection angle versus the frequency as well as with that estimated from the rise time and beam waist measurements.

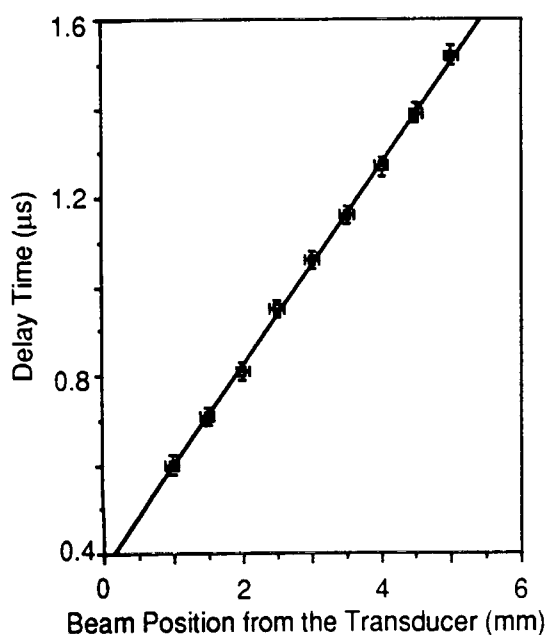


Figure 4. The measured delay time (left) between the RF pulse and the optical response and the optical pulse height (right) as a function of the optical beam position from the transducer.

The acoustic loss was estimated from the decay of the height of the optical response under pulsed operation as a function of the beam position from the transducer (figure 4). Because this decay is very small (maximum 3 %) we believe the value obtained (0.93 dB/cm) is an upper limit for the acoustic loss. For ultrasonic frequencies up to few hundreds of MHz the acoustic loss increases quadratically with the frequency according to Woodruff-Ehrenrich's equation:⁶

$$\alpha = 4\pi c\Gamma\gamma^2v^2\tau_p/3\rho v^3. \quad (1)$$

Here, c is the specific heat, γ is the effective Gruneisen parameter, v is the ultrasonic frequency and τ_p is the relaxation time of the lattice phonons. The relatively low ultrasonic loss observed is perhaps due to the relatively high acoustic velocity, the high density and short relaxation time. Low ultrasonic absorption means that the GLS glass systems are suitable also for high frequency AOMs. This helps to build GLS-AOMs operating in the Bragg regime with broader bandwidth and larger deflection angles, hence larger resolving power.

To determine the acousto-optic figures of merit, the experimental results of the diffraction efficiency in the 1st order Bragg diffraction (figure 1) were fitted to Gordon's^{4,5} formulae:

$$\eta = \sin^2(A(P_{rf})^{0.5}). \quad (2)$$

Here $A = \pi(\beta LM_2/2H)^{0.5}/\lambda$ with λ being the optical wavelength in vacuum, β is a factor which relates the acoustic power P_a transferred to the AO medium to the RF electrical power P_{rf} transferred to the transducer from the signal generator, $\beta = P_a/P_{rf}$, and $M_2 = n^6p^2/\rho v^3$, is the second AO figure of merit where p is the photoelastic (Pockel's) constant and ρ is the density. The fitted curve in figure 2 was obtained with $A = 0.531 W^{-0.5}$ which yields $\beta M_2 = 7.639 \times 10^{-15} \text{ sec}^3/\text{kg}$. The factor β was estimated from the Q-value of the transducer to be $\beta \approx 0.4$ which then yields $M_2 = 19 \times 10^{-15} \text{ sec}^3/\text{kg}$. From this value, the acoustic velocity, the refractive index and the density of the GLS glass we estimated the effective photoelastic constant and the other figures of merit $M_1 = n^7p^2/\rho v$, and $M_3 = n^7p^2/\rho v^2$. The

figures M_1 , M_2 , and M_3 represent scanning capability, diffraction efficiency, and resolution respectively.

4. Summary and Conclusions

Table 1 summarises the parameters of the GLS glass as an AO material. The high values of M_1 , M_2 , and M_3 indicate that the GLS glass is highly promising AO material for modulators and deflectors with wide bandwidth which together with the high acoustic velocity allows for fast switching and scanning. For the same type of AOM under consideration, we expect that a transducer length of 6 mm should give a diffraction efficiency larger than 70 % with 1 W RF power as shown in figure 2. This expectation was in fact confirmed experimentally using a transducer of 5 mm length.

Table 1
Acousto-optic parameters of the GLS glass

Optical transmission region (μm)	0.5 - 10
Refractive index (633 nm)	2.4
Density (g/cc)	4.1
Softening temperature ($^{\circ}\text{C}$)	561
Acoustic attenuation at 80 MHz (dB/cm)	0.93
Longitudinal acoustic velocity (m/s)	4375
Young's Modulus ($\times 10^{10}$ N/m ²)	7.84
Pockle's coefficient	0.18
M_1 ($\times 10^{-7}$ sm ² /kg)	8.7
M_2 ($\times 10^{-15}$ s ³ /kg)	19.0
M_3 ($\times 10^{-10}$ s ² m/kg)	2.0

We measured 75 % diffraction loss and 65 % diffraction efficiency under 1.5 W RF power. It should be noted here that under high frequencies, the diffraction efficiency into the 1st order Bragg diffraction should improve. This is because the acoustic velocity is high and therefore the acoustic wavelength Λ is larger for the same frequency, so that if either the transducer length is short or the operating frequency is low, in the tens of MHz range, additional diffraction peaks will appear due to Raman-Nath type diffraction. Hence, one should be

able to design Raman-Nath type AOMs using GLS glass since the criterion $2\pi\lambda L < n\Lambda^2$ can be easily fulfilled at low frequencies.

In conclusion, we have found that chalcogenide glasses based on Ga_2S_3 - La_2S_3 systems exhibit high acousto-optic figures of merit, high acoustic velocity and low acoustic losses. These properties of the GLS glass combined with its transparency both in the visible and the infrared, nontoxicity, high softening temperature, ease of fabrication, optical quality and isotropic nature, make it attractive for acousto-optic device applications.

Acknowledgements: This work was supported by a U.K. government (DTI) LINK project in collaboration with Gooch & Housego Ltd. The ORC is a U.K. government SERC sponsored Interdisciplinary Research Centre. We would like to thank Mr. D. Moreau, and Mr. G. Jones for useful interactions and discussions. The Ga_2S_3 and La_2S_3 powders were kindly supplied to us by Merck Ltd.

References

1. L.N. Magdich, V.Ya. Molchanov, *Acousto-optic Devices and their Applications*, Gordon & Breach Science Publishers, London, 1989.
2. J.T. Krause, C.R. Kurkjian, D.A. Pinnow, E.A. Sigety, *Appl. Phys. Lett.*, 17 (1970) 367.
3. A. Bornstein, J. Flahaut, M. Guittard, S. Jaulmes, A.M. Loireau - Lozac'h, G. Lucazeau, R. Reisfeld, in *The Rare Earths in Modern Science and Technology*, Ed. J.G. McCarthy, Plenum Press, N.Y., 1978, pp 99 - 606.
4. D.W. Hewak, R.S. Deol, J. Wang, G. Wylangowski, J.A. Mederios Neto, B.N. Samson, R.I. Laming, W.S. Brocklesby, D.N. Payne, A. Jha, M. Poulain, S. Otero, S. Surinach, M.D. Baró, *Elect. Lett.*, 29 (1993) 237.
5. D. Maydan, *IEEE J.Quant.Elect.*, QE-6 (1970) 223.
6. T.O. Woodruff, H. Ehrenreich, *Phys.Rev.*, 123 (1961) 1553.